NASA TECHNICAL NOTE

NASA TN D-5510

HOT-SALT STRESS-CORROSION OF A TITANIUM ALLOY UNDER A SIMULATED TURBINE-ENGINE COMPRESSOR ENVIRONMENT

by Hugh R. Gray and James R. Johnston

Lewis Research Center
Cleveland, Ohio

NATIONAL AERONAUTICS AND SPACE ADMINISTRATION • WASHINGTON, D. C. • OCTOBER 1969

1. Report No. NASA TN D-5510	2. Government Accession No.
3. Recipient's Catalog No.	
4. Title and Subtitle HOT-SALT STRESS-CORROSION OF A TITANIUM ALLOY UNDER A SIMULATED TURBINE-ENGINE COMPRESSOR ENVIRONMENT	5. Report Date October 1969
	6. Performing Organization Code
7. Author(s) Hugh R. Gray and James R. Johnston	8. Performing Organization Report No. E-5212
9. Performing Organization Name and Address Lewis Research Center National Aeronautics and Space Administration Cleveland, Ohio 44135	10. Work Unit No. 129-03
	11. Contract or Grant No.
	13. Type of Report and Period Covered Technical Note
12. Sponsoring Agency Name and Address National Aeronautics and Space Administration Washington, D. C. 20546	14. Sponsoring Agency Code

15. Supplementary Notes

16. Abstract

Threshold curves for hot-salt stress-corrosion of the Ti-8Al-1Mo-1V alloy were determined for a variety of exposure conditions that simulated the environment found in a compressor of a gas-turbine engine. Specimen surface condition was the most influential variable. Specimens in the as-machined condition exhibited higher threshold stresses than did stress-relieved specimens. High-velocity airflow and high air pressure raised the threshold curves for embrittlement slightly, but did not eliminate embrittlement entirely. Salt concentration, air dewpoint, and salt deposition temperature did not significantly shift threshold curves. Longer exposure times lowered threshold stresses.

17. Key Words (Suggested by Author(s)) Hot-salt stress-corrosion Titanium alloys Turbine-engine compressor environment Hydrogen embrittlement	18. Distribution Statement Unclassified - unlimited

19. Security Classif. (of this report)	20. Security Classif. (of this page)	21. No. of Pages	22. Price*
Unclassified	Unclassified	35	$3.00

*For sale by the Clearinghouse for Federal Scientific and Technical Information Springfield, Virginia 22151

HOT-SALT STRESS-CORROSION OF A TITANIUM ALLOY UNDER A SIMULATED TURBINE-ENGINE COMPRESSOR ENVIRONMENT

by Hugh R. Gray and James R. Johnston

Lewis Research Center

SUMMARY

Threshold curves for hot-salt stress-corrosion of the Ti-8Al-1Mo-1V alloy were determined for a variety of exposure conditions simulating the environment experienced in compressor components of aircraft gas-turbine engines operated in salt-air environments. The standard test procedure consisted of precoating the bore of each tubular specimen with salt in a dynamic air apparatus. Specimens were then exposed to salt-free air in the apparatus under various conditions of stress and airflow at 600° to 800° F (316° to 427° C) for 96 hours. After exposure, residual ductility was determined in a room-temperature tensile test at a constant crosshead speed of 0.005 inch per minute (0.01 cm/min). Embrittlement data are considered to be a more sensitive indication of hot-salt stress-corrosion than crack observations.

Specimen surface condition was the most influential variable. Stress-relieved specimens exhibited drastically lower threshold stresses than did as-machined specimens. However, the threshold curve exhibited by stress-relieved specimens occurred at such low stress levels that potentially detrimental variables could not be evaluated. Hence, the threshold curve for as-machined specimens was selected as the baseline to which the effects of all exposure variables were compared.

Embrittlement was decreased slightly, but not eliminated, when airstreams of 1100 feet per second (336 m/sec) or pressures of 52 psia (0.36 MN/m^2) were employed. In addition, salt deposition at elevated temperatures reduced the degree of embrittlement slightly.

Threshold curves for material coated with either 0.2 or 2 milligrams per square inch (0.03 or 0.3 mg/cm^2) salt were not significantly different. Increasing air dewpoint from -120° to 40° F (-84° to 4° C) did not systematically shift the threshold curve. Increasing the exposure time from 96 to 235 hours resulted in increased embrittlement.

The results of this investigation demonstrate that specimen surface condition exerts a considerable influence, and some exposure variables a slight influence, on threshold stresses. Thus, the danger of predicting the onset of hot-salt stress-corrosion with a unique threshold curve is illustrated.

INTRODUCTION

Laboratory investigations have demonstrated that titanium alloys exhibit embrittlement after exposure to halides while being stressed in the temperature range 500° to 900° F (260° to 482° C). This phenomenon has been termed hot-salt stress-corrosion. A recent investigation (ref. 1) has demonstrated conclusively that the quantities of salt deposited on compressor airfoils of commercial and military flight aircraft during typical operating conditions are in excess of the minimum amounts reported to cause embrittlement in laboratory tests.

Although the design stresses and temperatures of some current aircraft gas turbine components may be within the ranges where such embrittlement was observed in laboratory tests, no service failures have yet been reported that could be conclusively attributed to this phenomenon. The rationalization for the lack of service failures is not clear, although some investigators have postulated that engine environmental conditions, particularly high air velocities, high pressures, salt-air conditions, oil contamination and/or the unique cyclic operating conditions of an engine inhibit embrittlement.

A common laboratory test technique to establish if hot-salt stress-corrosion is occurring involves the exposure of statically loaded, heavily salt-coated specimens in a static air environment in the temperature range 500° to 900° F (260° to 482° C) for a specified time period, usually 100 hours. The exposed specimens are then examined for visual evidence of corrosion or cracking, and may also be subjected to mechanical testing, such as bend or tensile tests. The results are then interpreted on an embrittlement - no embrittlement basis. The boundary line on a plot of stress against temperature, separating regions of cracking from no cracking or embrittlement from no embrittlement, has been termed the threshold curve. Wide variations exist in threshold curves determined by various investigators because of differences in test conditions and the specific criteria used for defining hot-salt stress-corrosion. Obviously, those who define the onset of stress-corrosion as the visual appearance of cracks or corrosion products will report a different curve from those investigators concerned with catastrophic decreases in ductility.

Recently, it has been suggested (ref. 2) that the embrittlement observed in a titanium alloy after exposure conducive to hot-salt stress-corrosion is caused by hydrogen embrittlement. Direct measurements of increased hydrogen concentrations in fractured, exposed test specimens confirmed the hypothesis that hydrogen caused the temperature and strain-rate sensitive behavior observed in tensile tests of these specimens. Briefly, embrittlement was found to be most severe at slow strain rates and close to room temperature. As a result of the investigation of reference 2, we believe that room-temperature tensile testing at a constant crosshead speed of 0.005 inch per minute (0.01 cm/min) is a sensitive yet convenient method for determining the subtle influence of hydrogen. The dramatic influence of testing variables (reported in ref. 2) may also help

to account for a significant portion of the differences among reported threshold curves, since few, if any, of the previous investigators used the same or even similar testing procedures.

Only a limited number of investigations have been reported that deal with the influence of high-velocity airstreams on hot-salt stress-corrosion (refs. 3 and 4). These tests consisted of exposing heavily salt-coated, bend-type specimens in Mach 2.5 to 3 airstreams and then observing cracks and determining residual mechanical properties. In both of these cases, even though much of the predeposited salt spalled off during the short exposure periods, the tests demonstrated that the rapid airflow did not eliminate hot-salt stress-corrosion but that the degree of damage was generally less severe in high-velocity airstreams than in static air.

The effect of cyclic thermal exposure has been studied more extensively (refs. 3, 5, and 6). Generally, for constant total exposure times, less hot-salt stress-corrosion occurred for cyclic exposure than for continuous exposure. To our knowledge, no studies have yet been reported where both temperature and stress have been cycled. Since hydrogen has been confirmed as the embrittling agent (ref. 2), it is conceivable that stress cycling can influence the diffusion and microsegregation of hydrogen and, hence, reduce the severity of hot-salt stress-corrosion. However, threshold curve determinations under cyclic exposure conditions are not within the scope of this report.

In an effort to simulate actual turbine engine operating conditions more closely than previous investigations, a special test facility was designed. In this facility airflow, air pressure, air dewpoint, salt-in-air concentration, temperature and stress can be systematically controlled and their influence on hot-salt stress-corrosion evaluated. In addition, the influence of specimen surface preparation, salt deposition temperature, and salt concentration was determined. This report describes these effects for a titanium alloy and presents hot-salt stress-corrosion threshold data based on residual tensile ductility for one heat of this material under simulated engine exposure conditions.

MATERIALS, SPECIMENS, AND APPARATUS

Materials

A titanium - 8 aluminum - 1 molybdenum - 1 vanadium (Ti-8Al-1Mo-1V) alloy in the mill-annealed condition (1650^{o} F (899^{o} C) for 1 hr, water quenched) was used in this investigation. The chemical analysis and mechanical properties of the 1-inch- (2.5-cm-) diameter bar stock as reported by the manufacturer are as follows:

Chemical analysis, wt.%:	
Al	7.8
Mo	1.0
V	1.0
C	0.023
Fe	0.05
N	0.011
O	0.07
H	0.007
Ti	Balance
Yield strength, psi; MN/m^2	142 000; 978
Ultimate tensile strength, psi; MN/m^2	148 000; 1020
Elongation, percent	20
Reduction in area, percent	40

The mechanical properties determined at Lewis on machined specimens were an elongation of 18 percent, a reduction in area of 33 percent (based on outside diameter only), and an ultimate tensile strength of about 150 000 psi (1034 MN/m^2), which compare favorably with those given by the manufacturer.

Threshold curves and creep data from the literature (refs. 7 to 10), as well as a limited amount of creep and stress-rupture data determined at Lewis are presented in figure 1 and table I for reference purposes. These data are intended to be used only for

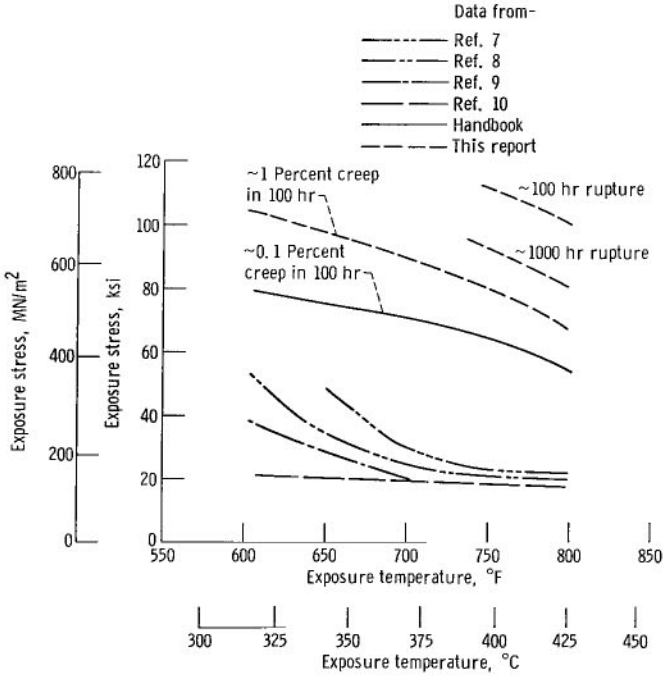

Figure 1. - Baseline creep, stress-rupture, and hot-salt stress-corrosion threshold data for Ti-8Al-1Mo-1V alloy (table I).

approximate representations of creep and stress-rupture curves.

Microstructural stability of this alloy has been demonstrated previously (ref. 2).

Specimens

Tubular tensile specimens of the type illustrated in figure 2 were employed in this investigation to determine both salt deposition data and threshold stresses for hot-salt

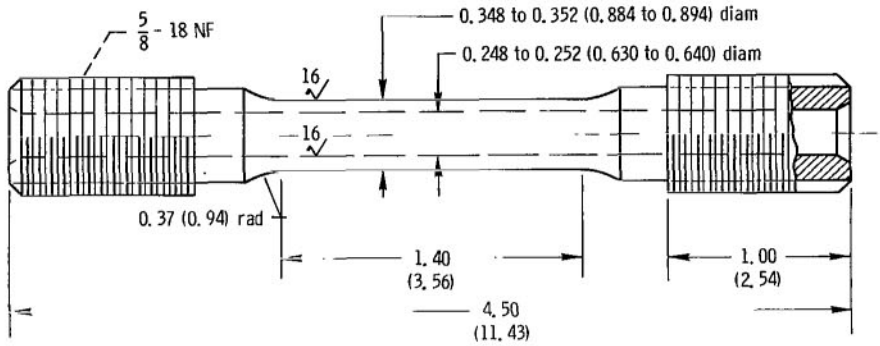

Figure 2. - Hollow, titanium alloy, tensile specimen used in hot-salt stress-corrosion investigation. (All dimensions are in inches (cm).)

stress-corrosion. All specimens were cleaned with acetone and distilled water immediately prior to use. The majority of specimens were used in the as-machined condition, with the rms surface finish less than 10 microinches (0.25 μm). One series of machined specimens was stress relieved by heat treatment at 1200° F (649° C) for 30 minutes in argon and then furnace cooled. Another series of machined specimens was stress relieved by chemical milling in a solution of 3-percent hydrofluoric acid, 30-percent nitric acid, and 67-percent water. Usually, 0.001 inch (0.002 cm) of metal was removed from all surfaces of these latter specimens. Neither of these stress-relieving treatments resulted in measurable changes in the mechanical properties of the specimens.

Apparatus

In order to simulate in the laboratory the salt-air environment and exposure conditions encountered by compressor airfoils during flight, a facility consisting of three dynamic air apparatuses of the type illustrated schematically in figure 3 was constructed. These apparatuses permit evaluation of the effects of salt-in-air concentration, airflow

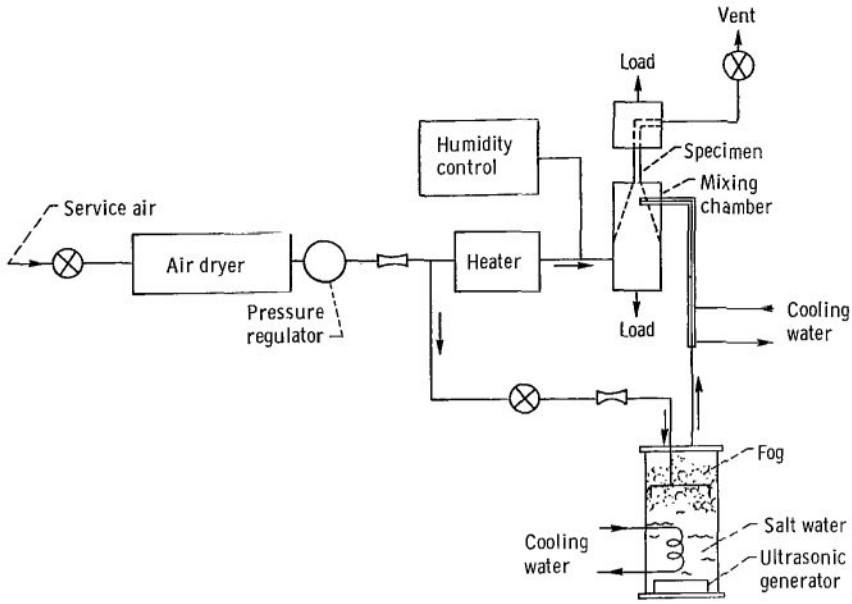

Figure 3. - Hot-salt stress-corrosion apparatus which simulates turbine-engine compressor operating conditions.

pressure, humidity, and specimen temperature and stress on the susceptibility of titanium alloys to hot-salt stress-corrosion.

The apparatus was operated as follows: service air was dryed to less than 1-part-per-million (ppm) volume-percent water, equivalent to a dewpoint of approximately -120° F (-84° C), heated to the test temperatures as high as 800° F (427° C), and rehumidified, if desired, before passing through the tubular specimen at a mass flow rate of approximately 120 pounds per hour (55 kg/hr). A small amount of this dry air (0.15 lb/hr or 68 g/hr) was diverted and first passed through a vessel containing ultrasonically generated salt-water fog with an average particle size of 1 micrometer and then injected continuously into the heated airstream just upstream of the specimen. Any desired concentration of salt-in-air was achieved by adjusting either the air mass flow rate, the salt-water concentration in the fog generator, or the salt-water usage rate.

TEST PROCEDURE

In most cases these tests were conducted in the following manner:

(1) The bore of each unstressed, tubular specimen was precoated with salt at 400° F (204° C) in the dynamic air apparatus to simulate the deposition conditions in an engine. (This method of precoating with salt is described in the section Salt Deposition.)

(2) These precoated specimens were then exposed to salt-free air in the dynamic air

apparatus for 96 hours under various conditions of temperature, stress, and airflow. (These conditions are described in the section Stress-Corrosion Exposure Conditions.)

(3) The specimens were then removed from the apparatus and the resultant embrittlement was determined by room-temperature tensile tests. (This test procedure is described in the section Tensile testing.)

Although most tests were made in this way, there were several exceptions to this procedure. These are as follows:

(1) One series of specimens was precoated with salt at 600° to 800° F (316° to 427° C) instead of at 400° F (204° C).

(2) One series of specimens was continuously coated with salt for the entire 96-hour exposure period instead of being precoated.

(3) One series of precoated specimens was exposed in a static air environment instead of in the dynamic air apparatus.

(4) One series of precoated specimens was exposed in the dynamic air apparatus for 235 hours instead of the standard 96 hours.

Salt Deposition

Precoat. - Most of the test specimens were precoated (prior to stress-corrosion testing) at 400° F (204° C) in the unstressed condition at salt-in-air concentrations and times chosen from the baseline data described latter in this section, to achieve average deposited salt concentrations ranging from approximately 0.2 to 2 milligrams per square inch (0.03 to 0.3 mg/cm^2). Some specimens were precoated with as much as 10 milligrams per square inch (1.6 mg/cm^2).

Continuous deposition. - One series of specimens was coated continuously while being stressed during the 96-hour exposure period at 600° to 800° F (316° to 427° C). Once again, the salt-in-air concentration and usage rate were adjusted in accordance with the baseline data. However, the air velocity and pressure were reduced slightly (table II) so that the ultrasonic fog generation system would function efficiently during the 96-hour test.

Baseline data. - In order to determine baseline salt deposition data, unstressed specimens were exposed for varying periods of time at several salt-in-air concentrations and temperatures. The influence of salt-in-air concentration on the average deposited salt concentration as a function of exposure time is presented in figure 4. For salt-in-air concentrations of 4, 40, and 400 parts per billion (ppb), the salt deposited on the specimens increased in a generally linear manner for any given time. These salt-in-air concentrations were obtained by increasing the salt-water concentration in the fog generator from 0.01- to 1-percent sodium chloride in distilled water. The salt-in-air

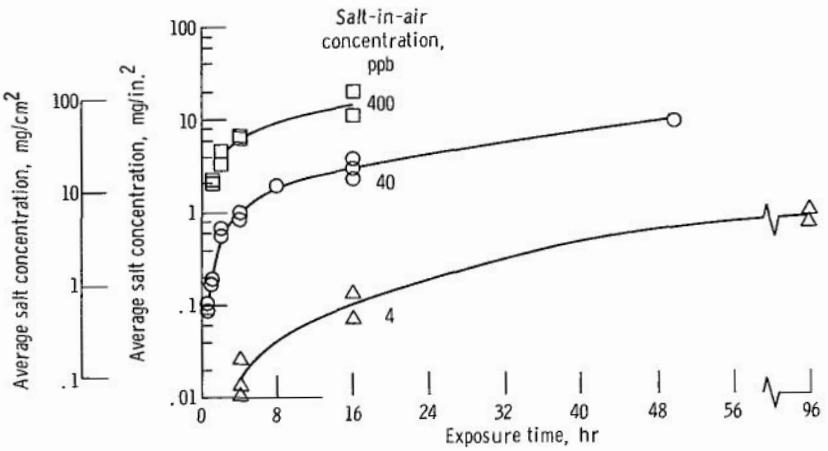

Figure 4. - Average salt deposition at 400° F (204° C) for three salt-in-air concentrations (table II). Air velocity, 1000 feet per second (305 m/sec); air pressure, 30 psia (0.21 MN/m^2).

concentration of 4 ppb represents typical seacoast environmental conditions during normal flying weather, while the 40-ppb concentration represents storm conditions (ref. 11). The airflow conditions during these deposition experiments are presented in table II.

The effect of deposition temperature is illustrated in figure 5. Less salt was deposited at the higher temperatures for a constant salt-in-air concentration of 40 ppb with all other experimental conditions similar to those previously described. Apparently, a

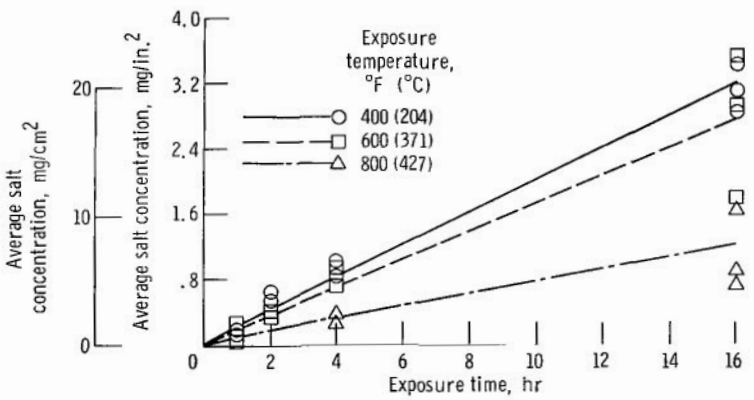

Figure 5. - Average salt deposition for three temperatures for a concentration of 40 ppb salt in air (table II). Air velocity, 1000 feet per second (305 m/sec); air pressure, 30 psia (0.21 MN/m^2).

greater proportion of the fog particles dryed out during transit at the higher temperatures and, hence, had a decreased probability of adhering to the specimen.

These deposition conditions provided a uniform dispersion of fine salt crystals on the bore of the specimen, as shown in figure 6.

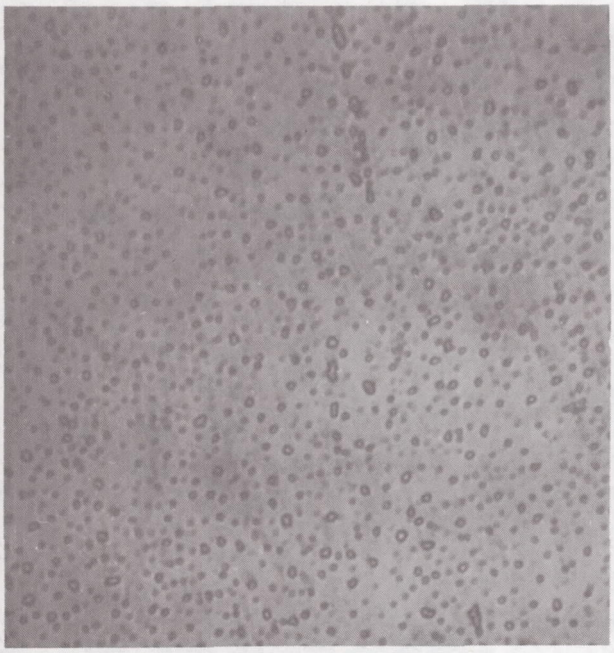

(a-1) Exposure time, 1 hour.

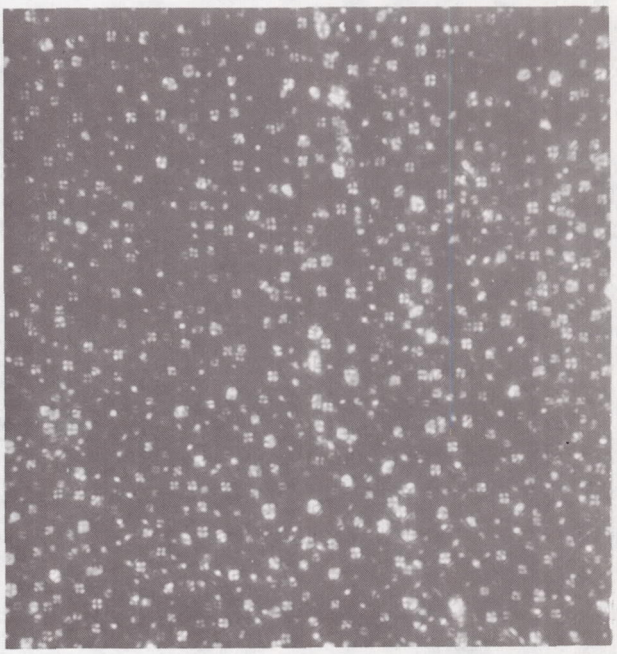

(b-1) Exposure time, 1 hour.

(a-2) Exposure time, 2 hours.

(a) Direct light.

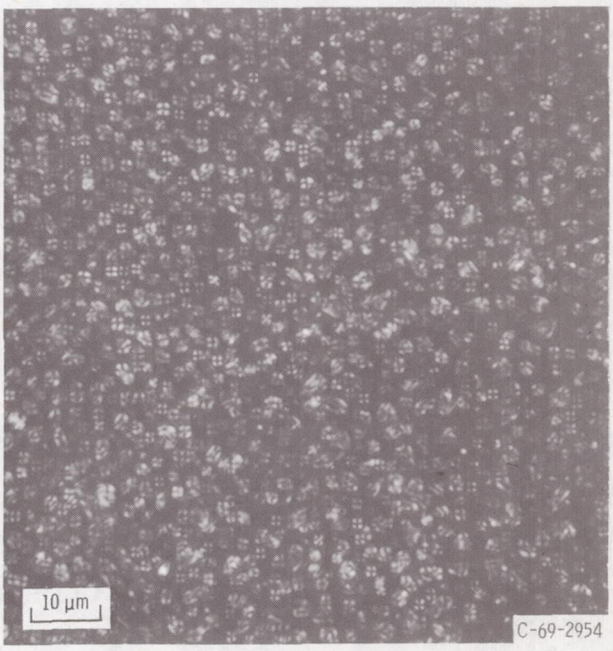

(b-2) Exposure time, 2 hours.

(b) Polarized light.

Figure 6. - Salt crystals deposited at 400° F (204° C). Salt-in-air concentration, 40 ppb; air velocity, 1000 feet per second (305 m/sec); air pressure, 30 psia (0.21 MN/m^2).

Stress-Corrosion Exposure Conditions

The standard test procedure was to expose specimens precoated with salt, as described previously, in the apparatuses to salt-free air at temperatures of 600°, 700°, and 800° F (316°, 371°, and 427° C) for approximately 96 hours. Several specimens were exposed at each temperature and the stresses applied ranged from 10 000 to 115 000 psi (69 to 792 MN/m^2). The standard exposure conditions used as a basis for comparing the effects of the variables considered were an air velocity of about 1100 feet per second (336 m/sec), an air pressure of 30 psia (0.21 MN/m^2), and an air dewpoint of -120° F (-84° C).

The influence of airflow was investigated by conducting tests in static air furnaces. The effect of air pressure was determined by conducting tests at 52 psia (0.36 MN/m^2). The effect of moisture in the air was studied by raising the air dewpoint to about 40° F (4° C) (5300 ppm water) in one series of tests by injecting distilled water into the heated airstream at a rate of 200 milliliter per hour. This corresponded to a relative humidity of 33 percent at 70° F (21° C). The effect of exposure time was studied by exposing two specimens for about 235 hours. All of these variables refer to calculated or measured exposure conditions at the specimen, which are listed in table III.

Postexposure Evaluation Methods

Tensile testing. - Subsequent to stress-corrosion exposure, all specimens were tensile tested at a constant crosshead speed of 0.005 inch per minute (0.01 cm/min) at room temperature. These tensile testing conditions had been determined (ref. 2) to provide high sensitivity to embrittlement and were also reasonably convenient to apply. Elongation was measured over a 1.00-inch (2.54-cm) gage length and apparent-reduction-in-area data were determined from changes only of the outside diameter of the tubular specimens.

Post-test inspection. - The fracture surfaces and bores of all specimens were examined for evidence of cracking under a microscope at 30×. Several specimens were also examined metallographically at 750×.

Measurement of deposited salt. - Concentrations of deposited salt were measured on the bore of each of the fractured specimen halves. The reported concentrations represent the average of the two halves. The measurements were made with a commercially available test strip for chlorides (ref. 12).

Interpretation of Embrittlement

Any specimen whose residual mechanical properties were significantly affected was classified as being above the threshold for hot-salt stress-corrosion, while unaffected properties placed a specimen below the threshold.

Embrittlement was assumed to occur if specimen elongation was less than 15 percent and reduction in area less than 25 percent. When both of these criteria are met, the data point is represented on threshold plots by a solid symbol. If one or both of these criteria are greater than the values stated, the specimen is considered to be unaffected by stress-corrosion and the data point is indicated by an open symbol. The fracture stress (based on the original area) was also indicative of the degree of embrittlement and is always recorded with the tabular data. The ultimate tensile strength of embrittled specimens was essentially unchanged from the as-received value.

Threshold curves were usually bracketed to within 10 000 psi (69 MN/m^2). On all threshold plots, the data points presented apply to the threshold curve represented by the solid line. Any threshold curve represented by a dashed line is given for comparative purposes.

RESULTS AND DISCUSSION

To briefly review, the standard test procedure consisted of precoating the bore of each tubular specimen with salt in a dynamic air apparatus, exposing the specimens to salt-free air and to various conditions of stress, temperature, and airflow, and then tensile testing at room temperature to determine residual ductility. The results obtained from these tests and from several variations of this test procedure are discussed in the following sections.

Appearance of Specimens after Stress-Corrosion Exposure

Inspection of all specimens after tensile testing revealed that heat-tinted cracks occurred on the fracture surfaces of a few specimens, as indicated in tables V, VIII, IX, and X. This type of oxidized or heat-tinted cracking definitely occurred during the hot-salt stress-corrosion exposure, and usually only at stress levels substantially above the threshold stress for embrittlement.

Additional small tears or cracks were frequently observed on the bore of specimens. However, it was concluded that these cracks did not originate during the expo-

sure period, but rather during tensile testing. This conclusion was determined on the following basis: all of these cracks were bright and shiny (no heat-tinting); cracks occurred close to the fracture plane and not elsewhere on the gage section; cracks were observed on unsalted specimens that had been exposed at elevated temperatures and subsequently tensile tested; cracks were observed almost as frequently and in about the same quantity on ductile as on brittle specimens. Hence, it was decided that the absence or presence of cracks of this nature was in no way an unequivocal indication of hot-salt stress-corrosion. These cracks were probably associated with a brittle surface oxide.

Effect of Specimen Surface Condition

Since baselines must be established for all succeeding experiments, the influence of surface preparation was studied. In addition to salting and exposure variables, it was felt that the manner of surface preparation may also be a factor contributing to the differences in literature threshold curves. Hence, a comparison of threshold curves for specimens in the as-machined and stress-relieved conditions was made. The threshold curve for as-machined specimens is presented in figure 7. This threshold was deter-

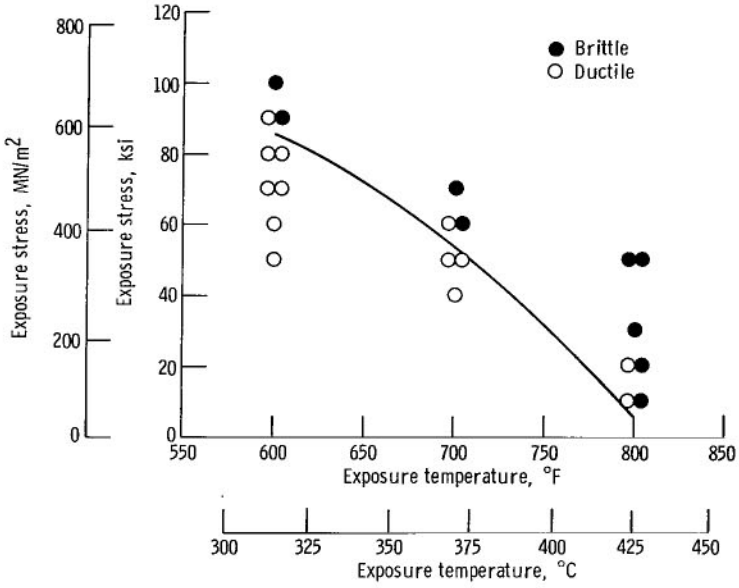

Figure 7. - Baseline threshold curve for as-machined specimens of Ti-8Al-1Mo-1V alloy (table IV). Specimens salt coated at 400° F (204° C); exposure time, 96 hours; air velocity, 1100 feet per second (336 m/sec); air pressure, 30 psia (0.21 MN/m^2); dewpoint, -120° F (-84° C).

mined with two separate batches of specimens (table IV). The good agreement indicates the specimens were machined reproducibly.

Stress relieving by heat treating. - A standard commercial stress-relief heat treatment (1200° F (649° C) for 30 minutes, and then furnace cooled in argon) was employed on a few machined specimens to study the influence of residual machining stresses on the embrittlement threshold (table V). Embrittlement was observed at stress levels as low as 30 000 psi (207 MN/m^2) at 600° F (316° C), compared to 90 000 psi (620 MN/m^2) in the as-machined condition. This lowering of the threshold stress is in the expected direction. Oxygen contamination of the surfaces of the specimens probably occurred during the high-temperature heat treatment, however, and contributed to the observed embrittlement of the base material. Hence, a meaningful threshold curve could not be obtained.

Precautions were made to minimize possible oxygen contamination by using high-purity argon and even encapsulating with getter foils in a few instances. However, the high affinity that titanium exhibits for oxygen nullified these precautions, as the specimens were usually abnormally tarnished after the stress-corrosion exposure period. Chemical analyses for oxygen in the surface layers appeared higher than normal but were so erratic that no conclusions could be made. Vacuum stress relieving was not employed because of the additional effect of reducing the hydrogen content of the base alloy, which, in itself, may influence susceptibility to hot-salt stress-corrosion.

Stress relieving by chemical milling. - In order to determine whether the relief of residual stresses was the important factor in the previously observed decrease in threshold stresses for heat-treated specimens, a chemical milling technique was also employed as a method for stress relieving.

Specimens were immersed and agitated in a solution of 3-percent hydrofluoric acid, 30-percent nitric acid, and 67-percent water. This composition was selected in order to minimize hydrogen contamination. A total of 0.001 inch (0.002 cm) of metal was usually removed from all surfaces of the specimens. The threshold curve exhibited by chemically milled specimens is presented in figure 8, along with the threshold curve for as-machined specimens for comparative purposes. It is felt that this threshold curve more truly represents the influence of residual surface stresses than did the threshold curve exhibited by specimens stress relieved by heat treating.

To confirm that the removal of 0.001 inch (0.002 cm) of metal from the surfaces of these specimens was sufficient to entirely eliminate the effects of residual stresses, a special pair of specimens was tested. One specimen was chemically milled only 0.0005 inch (0.001 cm) and then exposed at a stress level just above the previously determined threshold stress at 600° F (316° C) for specimens chemically milled 0.001 inch (0.002 cm). Another specimen was chemically milled 0.002 inch (0.005 cm) and then exposed at a stress level just below the threshold stress at 600° F (316° C). The

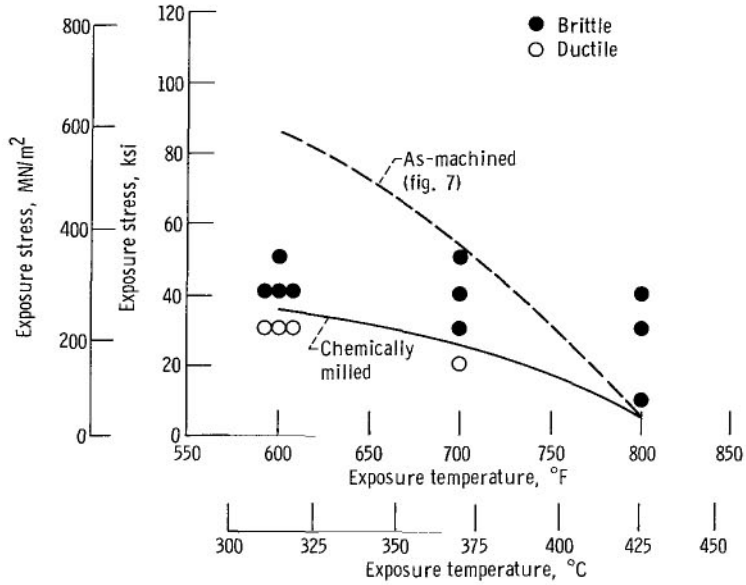

Figure 8. - Effect of specimen surface condition on threshold curve (table V). Specimens salt coated at 400° F (204° C); exposure time, 96 hours; air velocity, 1100 feet per second (336 m/sec); air pressure, 30 psia (0.21 MN/m^2); dewpoint, -120° F (-84° C).

threshold stress remained unchanged, thus demonstrating that the standard amount of metal removal of 0.001 inch (0.002 cm) was more than sufficient to eliminate all effects of residual surface stresses (fig. 8 and table V).

The influence of low-temperature oxidation subsequent to chemical milling was investigated by comparing one specimen that had been exposed to ambient air for 4 weeks and another specimen exposed to 400° F (204° C) air for 2 hours with specimens that were tested soon after chemical milling, the usual procedure. The threshold stress was not raised by either of these variations (fig. 8 and table V), thus demonstrating that the natural oxide forms quickly on titanium alloys and that these oxidation conditions had no effect on subsequent embrittlement.

Chemical milling may have produced some secondary effects, such as grain boundary etching and hydrogen contamination, although no excess hydrogen could be detected by vacuum fusion techniques. Electropolishing techniques, which would have been more certain to minimize these hazards, were not employed because of the experimental difficulties associated with the tubular specimen design.

The fact that the threshold curves were lower for stress-relieved than for as-machined specimens suggests that the surface stresses resulting from machining were compressive, with a magnitude of about 50 000 psi (345 MN/m^2). X-ray techniques were attempted, without success, to confirm the magnitude and sign of the residual stresses. However, the assumptions cited regarding these stresses are compatible with the obser-

vations of another investigation (ref. 3) in which mechanically induced (glass-bead peening and vibratory cleaning techniques) residual compressive stresses were determined to be effective in preventing or alleviating hot-salt stress-corrosion of the Ti-8Al-1Mo-1V alloy. Another investigation (ref. 13) has indicated that compressive stresses up to approximately 120 000 psi (827 MN/m^2) can result from glass-bead peening but are usually no deeper than 0.001 inch (0.002 cm). Of course, some types of machining operations could introduce residual tensile stresses in specimens of different configurations. In those instances, the threshold curve for specimens with residual tensile surface stresses could be expected to occur at lower stress levels than if the same specimens were in the stress-relieved condition.

Since the threshold curve exhibited by specimens in the chemically milled condition occurred at such low stress levels, the influence of any potentially detrimental exposure variables could not be accurately evaluated. Consequently, the effects of air velocity, air dewpoint, and salt concentration could not be determined in a meaningful fashion.

However, the threshold curve exhibited by specimens in the as-machined condition occurred at intermediate stress levels so that the effects of both detrimental and beneficial exposure variables could be investigated. Consequently, this threshold curve was used as the baseline or standard to which all other threshold curves are compared. In addition, the influence of most exposure variables was spot-checked on specimens in the chemically milled condition and the results are discussed briefly in each subsequent section of this report. These spot-check data are not represented on any of the figures in this report although they are presented in the tables.

Effect of Airflow

In order to evaluate the influence of airflow during the exposure of specimens precoated in the usual manner, the standard threshold curve determined at an air velocity of 1100 feet per second (336 m/sec) was compared with the threshold curve obtained for a static air environment typical of laboratory furnaces. The influence of airflow is apparent in figure 9, where the threshold curve determined in static air occurs at relatively low stress levels, more nearly comparable to the upper curves from the literature data presented earlier in figure 1. The static-air-environment threshold data are given in table VI.

At the high airflow, higher stresses were required before the embrittlement threshold was reached. The influence of airflow is most significant at the lower end of the temperature range investigated, 600° F (316° C), with a diminishing influence apparent at 700° F (371° C). No effect of airflow was observed at 800° F (427° C). For specimens in the chemically milled condition, no effect of airflow was observed. The thresh-

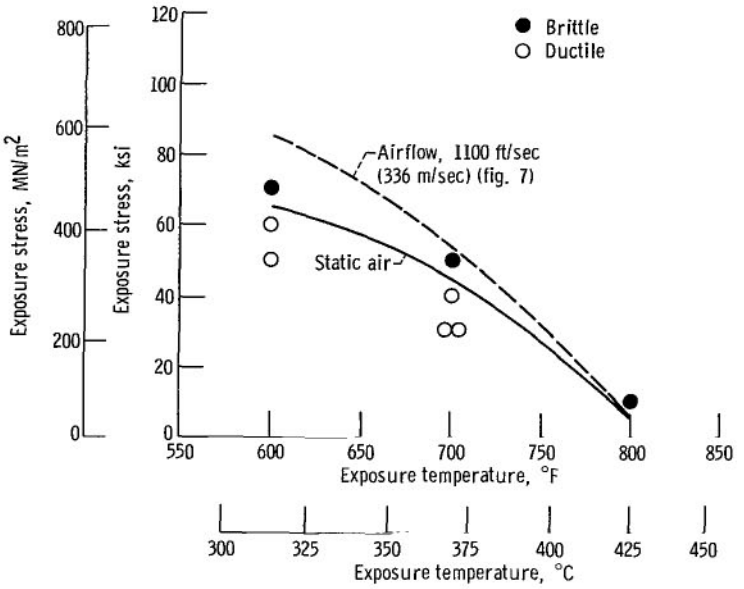

Figure 9. - Effect of airflow on threshold curve (table VI). As-machined specimens salt-coated at 400° F (204° C); exposure time, 96 hours; static air ambient pressure and dewpoint.

old stress at 600° F (316° C) remained above 30 000 psi (207 MN/m^2) for both static (table VI) and flowing air environments (table V).

These results would indicate that a gaseous corrosion product may be involved at some stage of the hot-salt stress-corrosion process. High-velocity airstreams may sweep away some of this phase and help to decrease, but not eliminate, embrittlement at lower exposure temperatures. It is also possible that the higher threshold stress at low temperatures may be due to repassivation of the specimen surface because of the increased availability of oxygen in the dynamic air environment. However, the corrosion kinetics at the high exposure temperature are apparently so rapid that even a high-velocity airstream does not offer any beneficial effect.

Effect of Air Pressure

To determine the influence of air pressure on susceptibility to hot-salt stress-corrosion, a pressure of 52 psia (0.36 MN/m^2) was used in one series of tests. By increasing the inlet air pressure and mass flow, this higher pressure could be obtained together with a relatively high-velocity airstream of 800 feet per second (240 m/sec), which is comparable with the 1100-foot-per-second (336-m/sec) velocity at 30 psia (0.21 MN/m^2) employed as the standard exposure conditions. As evident from figure 10, the higher pressure increased the threshold stress, principally at the lower

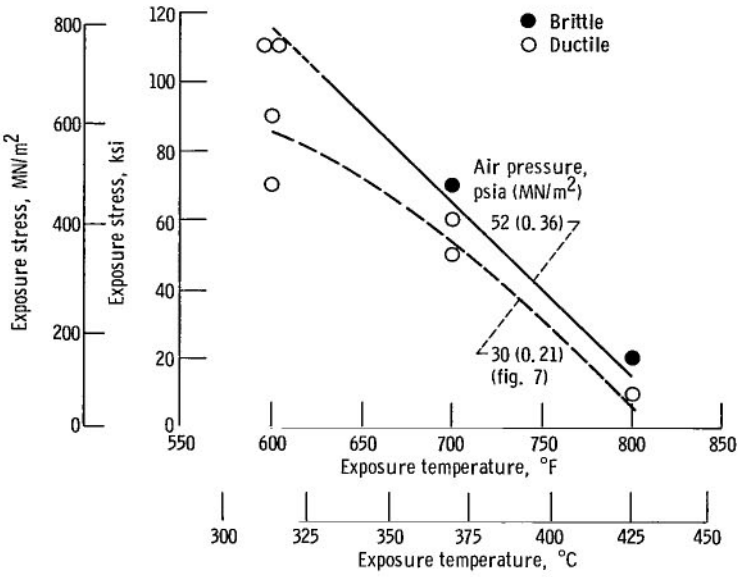

Figure 10. - Effect of air pressure on threshold curve (table VII). As-machined specimens salt-coated at 400° F (204° C); exposure time, 96 hours; air velocity, 800 feet per second (240 m/sec); air pressure, 52 psia (0.36 MN/m^2); dewpoint, -120° F (-84° C).

temperature of 600° F (316° C), with the stress level for embrittlement somewhat above 110 000 psi (758 MN/m^2). Specimens were not found to be brittle at this temperature and stress. Creep limitations precluded meaningful threshold data above this stress level. These threshold data are given in table VII. The beneficial effect of high air pressure was also observed on specimens tested in the chemically milled condition. The threshold stress at 600° F (316° C) was raised about 10 000 psi (69 MN/m^2) (compare table VII and table V).

This beneficial influence of high air pressure is not fully understood, although it may be possible that the chemical corrosion reactions that produce embrittling hydrogen have been inhibited in some manner. The increased availability of oxygen may result in rapid repair of the naturally protective surface oxide, thus minimizing embrittlement at 600° F (316° C). Obviously, additional research is required to clarify the beneficial influence of high air pressure on the susceptibility of titanium alloys to hot-salt stress-corrosion.

Effect of Moisture

Two different air dewpoints were used in an effort to determine the effect of environmental moisture on hot-salt stress-corrosion. The standard exposure test was

conducted with air dryed to a dewpoint of -120° F (-84° C), or less than 1 ppm water. The rate at which moisture passed through the specimen was about 0.01 milliliter per hour during the exposure period. The dewpoint was raised to about 40° F (4° C) by continuously injecting approximately 220 milliliter per hour of distilled water into the heated airstream, thereby raising the moisture content to 5300 ppm.

These significantly different moisture levels did not produce any consistent effect on the threshold stress levels (fig. 11). The threshold data for the high-dewpoint air

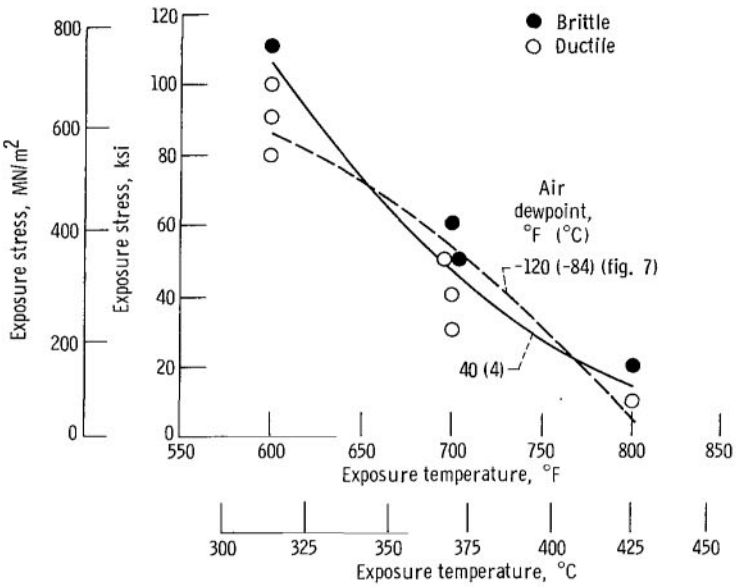

Figure 11. - Effect of air dewpoint on threshold curve (table VIII). As-machined specimens salt-coated at 400° F (204° C); exposure time, 96 hours; air velocity, 1100 feet per second (336 m/sec); air pressure, 30 psia (0.21 MN/m²); dewpoint, 40° F (4° C).

are given in table VIII. For example, at 600° F (316° C) the threshold stress for the moist-air environment was slightly higher than for dry air, whereas at 700° F (371° C) the threshold stress was slightly lower. Similarly, the threshold stress at 600° F (316° C) was unchanged for a chemically milled specimen exposed to the high-dewpoint air environment (compare table VIII and table V).

It is difficult to explain this seemingly erratic behavior, especially in view of the numerous experiments in the literature (refs. 3, 10, and 14) which report increased hot-salt stress-corrosion with increasing moisture concentration in the environment. It is possible that these results represent experimental scatter, although the appearance of heat-tinted cracks on fracture surfaces of specimens exposed to the higher dewpoint air at relatively low stress levels at 700° F (371° C) (table VIII) seems to agree with the general observations reported in the literature.

Apparently, if there is any critical moisture level required for the initiation of hot-salt stress-corrosion, then that concentration has already been exceeded in the dry-air environment (<1 ppm water). It is important to note that enough water may have been retained in inclusions in the salt crystals originally deposited to cause hot-salt stress-corrosion (ref. 15).

Effect of Salt Concentration

A recent investigation (ref. 1) indicated that average salt concentrations of about 0.1 milligram per square inch (0.02 mg/cm^2) are deposited on compressor airfoils of engines used in transoceanic flight and about 1 milligram per square inch (0.2 mg/cm^2) is deposited on compressor airfoils after exposure to severe salt-air environments. These concentrations are considerably in excess of the minimum amounts reported to have caused embrittlement in laboratory tests.

A loss of ductility has been reported (ref. 11) in a titanium alloy with a salt coating of 0.05 milligram per square inch (0.008 mg/cm^2) after exposure to stress and temperature in a laboratory test. A chloride concentration equivalent to a concentration of sodium chloride as little as 0.033 milligram per square inch (0.005 mg/cm^2) has also been reported to cause cracking of the Ti-8Al-1Mo-1V alloy (ref. 16).

Consequently, the influence of salt concentration on the stress-corrosion threshold

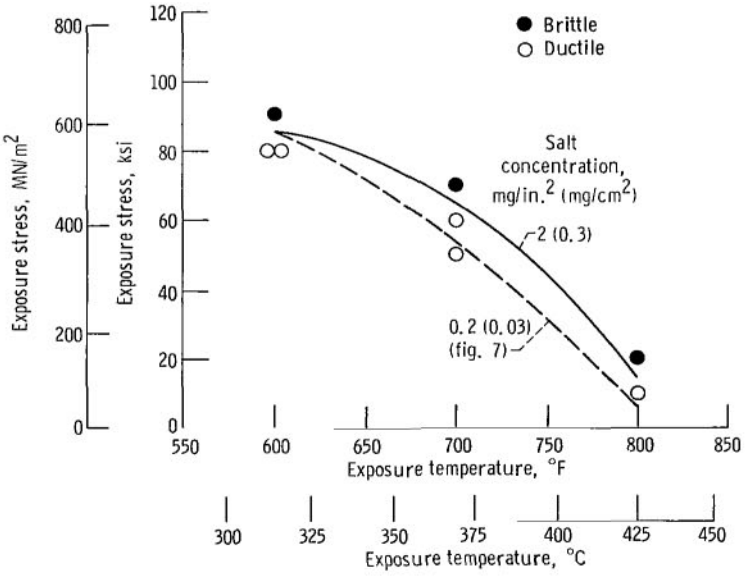

Figure 12. - Effect of salt concentration on threshold curve (table IX). As-machined specimens salt-coated at 400° F (204° C); exposure time, 96 hours; air velocity, 1100 feet per second (336 m/sec); air pressure, 30 psia (0.21 MN/m^2); dewpoint, -120° F (-84° C).

was studied in this investigation by comparing the threshold curves obtained with coatings of nominally 0.2 and 2 milligrams per square inch (0.03 and 0.3 mg/cm^2). It is evident from figure 12 that susceptibility to hot-salt stress-corrosion was essentially unchanged for this tenfold increase in salt concentration. Threshold data for specimens with high salt concentrations are given in table IX. Even an extremely heavy salt concentration of 10 milligrams per square inch (1.5 mg/cm^2) did not lower the threshold stress in the static air environment at 700° F (371° C) (table VI). Similarly, no significant influence of salt concentration was observed at 600° F (316° C) for a specimen in the chemically milled condition (compare table IX and table V).

It is possible that some protection may be afforded by heavier salt deposits, which, since they consist of a uniform and continuous deposit of salt crystals, may inhibit the ready ingress of two of the vital ingredients in the corrosion process, water and oxygen. Previous experiments (refs. 14, 17, and 18) have demonstrated that light salt coatings are more detrimental than heavy coatings. The rationalization for this effect may be the greater availability of moisture and oxygen in the case of the light coatings.

Effect of Salt Deposition Temperature

The influence of salt deposition temperature was investigated by comparing threshold curves of specimens precoated at 400° F (204° C) with specimens precoated at the exposure temperatures of 600°, 700°, and 800° F (316°, 371°, and 427° C). As evident from the threshold data presented in figure 13, precoating at both 600° and 700° F (316° and 371° C) resulted in decreased embrittlement, that is, a higher threshold stress. However, the degree of embrittlement observed at 800° F (427° C) was similar for specimens precoated at either 400° or 800° F (204° or 427° C). The elevated-temperature threshold data are given in table X. A slightly higher threshold stress was also observed for chemically milled specimens precoated at 600° F (316° C) (compare table X and table V).

It is probable that precoating specimens at moderately elevated temperatures results in a decreased amount of moisture being retained in the salt crystals, compared to specimens coated at 400° F (204° C). Hence, the former have less susceptibility to hot-salt stress-corrosion. Water, in the form of inclusions in salt crystals (ref. 15), has been shown to be a necessary ingredient in the corrosion process (refs. 10, 14, and 15). Experiments with predryed salt have indicated decreased susceptibility to corrosion, thereby confirming the role of water (refs. 10 and 19). On the other hand, the corrosion kinetics at 800° F (427° C) may be so rapid that slight changes in water concentration may not be so critical. In this way the similar degrees of embrittlement observed in specimens precoated at 400° F (204° C) and at 800° F (427° C) can be rationalized.

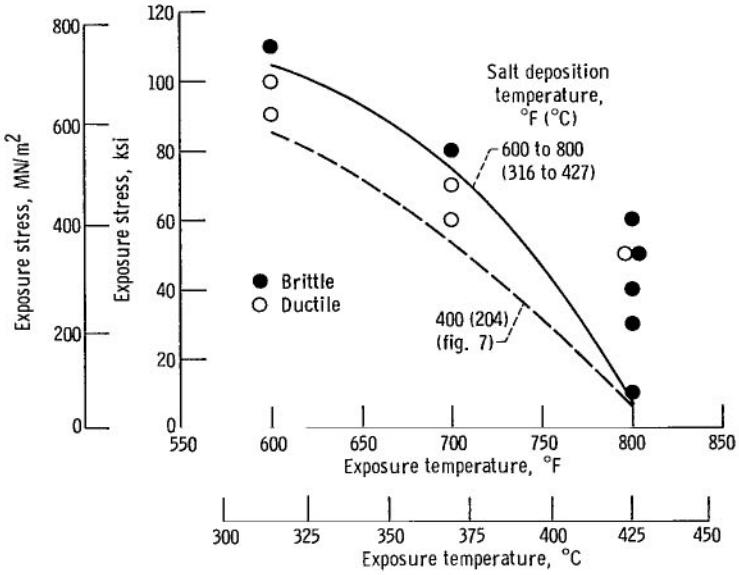

Figure 13. - Effect of salt deposition temperature on threshold curve (table X). As-machined specimens; salt deposition temperature, 600° to 800° F (316° to 427° C); exposure time, 96 hours; air velocity, 1100 feet per second (336 m/sec); air pressure, 30 psia (0.21 MN/m^2); dewpoint, -120° F (-84° C).

Effect of Salt Deposition Technique

The influence on subsequent embrittlement of precoating as opposed to continuous coating with salt was determined. Specimens were salted while being stressed over the entire threshold range at the exposure temperatures of 600° to 800° F (316° to 427° C) by continuously injecting salt-fog into the main airstream during the entire 96-hour exposure period. The specimens were uncoated prior to this exposure. This threshold curve was then compared in figure 14 with that determined with precoated specimens salted at various exposure temperatures. In most cases the two coating techniques resulted in approximately equal salt concentrations. The continuous-salt-deposition threshold data are given in table XI.

Similar threshold stresses were measured for both precoated and continuously coated specimens at both 600° and 700° F (316° and 371° C). The minor variations observed at these temperatures are not considered significant. However, a substantial difference in threshold stress was observed at the highest exposure temperature of 800° F (427° C). The threshold stress for the continuously salted material was about 50 000 psi (345 MN/m^2) compared to a threshold stress of only about 5000 psi (35 MN/m^2) for the precoated material. A possible rationalization for this behavior is that a significant degree of surface oxidation may have occurred during the early stages of the exposure period, before sufficient salt was deposited, thus affording a

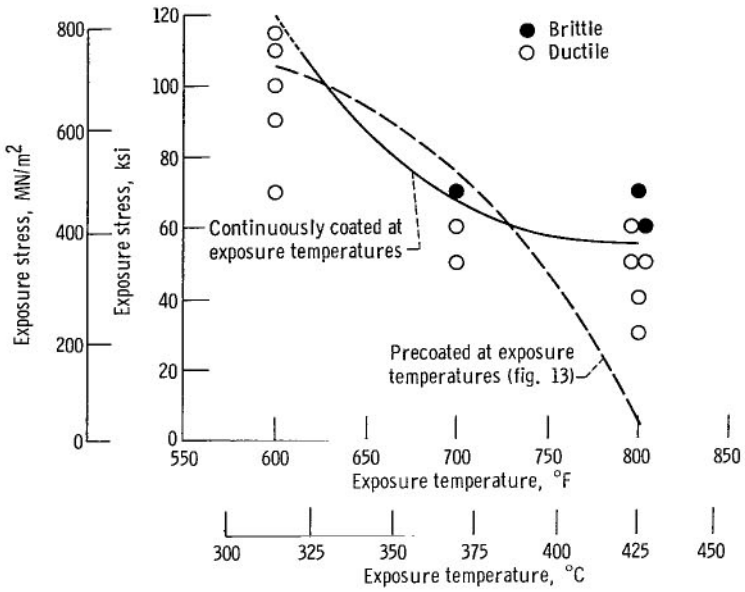

Figure 14. - Effect of salt deposition technique on threshold curve (table XI). As-machined specimens; exposure time, 96 hours; air velocity, 1050 feet per second (320 m/sec); air pressure, 25 psia (0.17 MN/m^2); dewpoint, -120° F (-84° C).

beneficial protective oxide. Additional investigation is required to substantiate this concept.

Once again the relatively small influence of heavy salt concentrations was confirmed in these experiments, where, in several cases, very heavy salt deposits did not shift the threshold curve (table XI).

Effect of Exposure Time

As might be expected, threshold stresses for any given temperature are dependent on the exposure time (refs. 3 and 7). The vast majority of investigations have been concerned with 100-hour threshold curve determinations. However, one exposure condition was selected in this investigation to spot-check the effect of exposure time. For example, a limited amount of data determined with precoated specimens at 600° F (316° C) indicated that the threshold stress decreased from about 85 000 to approximately 60 000 psi (587 to 414 MN/m^2) when the exposure time was increased from the standard 96 hours to about 235 hours (table XII). These tests demonstrate the importance of considering exposure times in all stress-corrosion threshold determinations.

CONCLUDING REMARKS

Once again, it should be emphasized that threshold curves determined from embrittlement data are considered to be a more sensitive indication of the subtle influence of hydrogen resulting from the hot-salt stress-corrosion phenomenon than are threshold curves based on crack observations.

The most important conclusion to be drawn from this investigation of exposure variables is that no unique threshold curve can be predicted for design use. There is a wide range of stress levels at any given temperature where embrittlement may be encountered. This is due to the myriad of variables than can affect the stress-corrosion process, ranging from specimen preparation through environmental exposure conditions to testing criteria.

Although only the Ti-8Al-1Mo-1V alloy was considered in this investigation, it is probable that other $\alpha + \beta$ titanium alloys will exhibit similar trends in threshold with changing exposure variables. The exact degree of shift in threshold curves may not be identical to the data determined in this investigation. Additional studies are required to substantiate this concept. Likewise, the influence of exposure variables must be determined for single-phase α and β alloys.

SUMMARY OF RESULTS

Threshold curves for hot-salt stress-corrosion of the Ti-8Al-1Mo-1V alloy were determined for a variety of exposure conditions that simulated the environment normally found in gas-turbine engine compressors operating in salt-air environments. The standard test procedure consisted of precoating the bore of each tubular specimen with salt in a dynamic air apparatus. Specimens were then exposed to salt-free air in the apparatus under various conditions of stress and airflow in the temperature range 600° to 800° F (316° to 427° C) for 96 hours. After exposure, residual ductility was determined in a room-temperature tensile test at a constant crosshead speed of 0.005 inch per minute (0.01 cm/min). If a specimen exhibited less than 25 percent reduction in area and less than 15 percent elongation, it was considered to be embrittled. If both of these criteria were not met, the specimen was considered to be ductile.

The threshold curve for specimens in the stress-relieved condition occurred at such low stress levels that potentially detrimental exposure variables could not be accurately evaluated. Hence, the threshold curve exhibited by specimens in the as-machined condition was selected as the baseline for all subsequent comparisons of the effects of exposure variables.

The results of these tests are as follows:

1. Specimen surface condition had a dramatic influence on threshold curves. Specimens that had been stress-relieved exhibited significantly lower threshold stresses for embrittlement that did specimens tested in the as-machined condition.

2. An air velocity of 1100 feet per second (336 m/sec) resulted in a higher stress for embrittlement than did static air, especially at 600° F (316° C).

3. Increasing the air pressure from 30 to 52 psia (0.21 to 0.36 MN/m^2) also resulted in decreased hot-salt stress-corrosion at 600° F (316° C), that is, a higher stress for embrittlement.

4. Dewpoint ranges from -120° to 40° F (-84° to 4° C) did not significantly influence the threshold stresses at any of the exposure temperatures, thus indicating that even the small amount of moisture contained in the dry air was sufficient to sustain the hot-salt stress-corrosion reaction.

5. Threshold curves were not significantly affected by salt concentrations ranging from about 0.2 to 2 milligrams per square inch (0.03 to 0.3 mg/cm^2).

6. Specimens precoated at 600° and 700° F (316° and 371° C) exhibited slightly higher threshold stresses than did specimens precoated at 400° F (204° C).

7. Continuous coating with salt during the 96-hour exposure period resulted in a substantially higher threshold stress at 800° F (427° C) than did precoating. This elevation of the threshold curve may be associated with the protective effect afforded by a preoxidized specimen surface which could have occurred at the high exposure temperature before a significant amount of salt was deposited.

8. The threshold stress at 600° F (316° C) was reduced by about 25 000 psi (173 MN/m^2) when the exposure time was increased from 96 to 235 hours.

Lewis Research Center,
National Aeronautics and Space Administration,
Cleveland, Ohio, August 25, 1969,
129-03.

REFERENCES

1. Ashbrook, Richard L.: A Survey of Salt Deposits in Compressors of Flight Gas Turbine Engines. NASA TN D-4999, 1969.

2. Gray, Hugh R.: Hot-Salt Stress-Corrosion of Titanium Alloys: Generation of Hydrogen and Its Embrittling Effect. NASA TN D-5000, 1969.

3. Heimerl, G. J.; Braski, D. N.; Royster, D. M.; and Dexter, H. B.: Salt Stress Corrosion of Ti-8Al-1Mo-1V Alloy Sheet at Elevated Temperatures. Stress-Corrosion Cracking of Titanium. Spec. Tech. Publ. No. 397, ASTM, 1966, pp. 194-214.

4. Weber, K. E.; and Davis, A. O.: Stress Corrosion of Titanium Alloys Under Simulated Supersonic Flight Conditions. NASA CR-981, 1967.

5. Stone, L. H.; and Freedman, A. H.: Cyclic Hot-Salt Stress Corrosion of Titanium Alloys. Rep. NOR-67-151, Northrop Corp. (AFML-TR-67-289), Sept. 1967. (Available from DDC as AD-825239.)

6. Piper, D. E.; and Fager, D. N.: The Relative Stress-Corrosion Susceptibility of Titanium Alloys in the Presence of Hot Salt. Stress-Corrosion Cracking of Titanium. Spec. Tech. Publ. No. 397, ASTM, 1966, pp. 31-52.

7. Donachie, M. J., Jr.; Danesi, W. P.; and Pinkowish, A. A.: Effects of Salt Atmosphere on Crack Sensitivity of Commercial Alloys at 600 to 900 F. Stress-Corrosion Cracking of Titanium. Spec. Tech. Publ. No. 397, ASTM, 1966, pp. 179-193.

8. Turley, R. V.; and Avery, C. H.: Elevated-Temperature Static and Dynamic Sea-Salt Stress Cracking of Titanium Alloys. Stress-Corrosion Cracking of Titanium. Spec. Tech. Publ. No. 397, ASTM, 1966, pp. 1-30.

9. Boyd, W. K.; and Fink, F. W.: The Phenomenon of Hot-Salt Stress-Corrosion Cracking of Titanium Alloys. NASA CR-117, 1964.

10. Hatch, A. J.; Rosenberg, H. W.; and Erbin, E. F.: Effects of Environment on Cracking in Titanium Alloys. Stress-Corrosion Cracking of Titanium. Spec. Tech. Publ. No. 397, ASTM, 1966, pp. 122-136.

11. Boudreau, J. S.; Green, H. M.; and Puffer, D. W.: Stress Corrosion Behavior of Titanium Alloy 6-2-4-2 As Related to Engine Operation. Proceedings 8th Annual National Conference on Environmental Effects of Aircraft and Propulsion Systems. Inst. Environmental Sci., 1968, pp. 105-122.

12. Anon.: Quantab Chloride Titrators. Pamphlet 1104AD R636, Ames Co., Div. of Miles Laboratories Inc., Elkhart, Ind., 1966.

13. Braski, David N.; and Royster, Dick M.: X-Ray Measurement of Residual Stresses in Titanium Alloy Sheet. Presented at 15th Annual Conference on Applications of X-Ray Analysis, Denver, Colo., Aug. 10-12, 1966.

14. Logan, H. L.; McBee, M. J.; Bechtoldt, C. J.; Sanderson, B. T.; and Ugiansky, G. M.: Chemical and Physical Mechanisms of Salt Stress-Corrosion Cracking in the Titanium 8-1-1 Alloy. Stress-Corrosion Cracking of Titanium. Spec. Tech. Publ. No. 397, ASTM, 1966, pp. 215-229.

15. Rideout, S. P.; Louthan, M. R.; Jr.; and Selby, C. L.: Basic Mechanisms of Stress-Corrosion Cracking of Titanium. Stress-Corrosion Cracking of Titanium. Spec. Tech. Publ. No. 397, ASTM, 1966, pp. 137-151.

16. Seastrom, C. C.; and Gorski, R. A.: The Influence of Fluorocarbon Solvents on Titanium Alloys. Accelerated Crack Propagation of Titanium by Methanol, Halogenated Hydrocarbons, and Other Solutions. DMIC Memo 228, Battelle Memorial Inst., Mar. 6, 1967, pp. 20-28. (Available from DDC as AD-825607.)

17. Braski, David N.: Preliminary Investigation of Effect of Environmental Factors on Salt Stress Corrosion Cracking of Ti-8Al-1Mo-1V at Elevated Temperatures. NASA TM X-1048, 1964.

18. Simenz, R. F.; Van Orden, J. M.; and Wald, G. G.: Environmental Effects Studies on Selected Titanium Alloys. Stress-Corrosion Cracking of Titanium. Spec. Tech. Publ. No. 397, ASTM, 1966, pp. 53-79.

19. Rideout, S. P.; Ondrejcin, R. S.; Louthan, M. R.; and Rawl, D. E.: The Role of Moisture and Hydrogen in Hot-Salt Cracking of Titanium Alloys. Presented at Conference on Fundamental Aspects of Stress Corrosion Cracking, Ohio State Univ., Sept. 1967.

TABLE I. - BASELINE CREEP AND STRESS-RUPTURE

PROPERTIES OF Ti-8Al-1Mo-1V ALLOY

Specimen	Exposure conditions					Creep and stress-rupture data	
	Temperature		Time, hr	Stress		Reduction in area, percent	Elongation, percent
	°F	°C		ksi	MN/m^2		
116	600	316	93	110	758	1.7	--
266	↓	↓	94	↓	↓	1.8	--
243			96			2.0	--
44			112			3.8	--
112			96	115	792	3.8	--
263	700	371	96	90	620	.6	--
267	800	427	95	60	414	.6	--
104			97	70	482	1.2	--
115			1055	80	551	51 (rupture)	28
46			116	100	689	45 (rupture)	17

TABLE II. - SALTING CONDITIONS

[Air dewpoint, -120° F (-84° C).]

Type of experiment	Temperature		Airflow					
			Mass flow		Velocity		Pressure	
	°F	°C	lb/hr	kg/hr	ft/sec	m/sec	psia	MN/m^2
Baseline deposition:								
Salt-in-air concentration (fig. 4)	400	204	120	55	1000	305	30	0.21
Deposition temperature (fig. 5)	400 to 800	204 to 427	100 to 120	45 to 55	1000 to 1200	305 to 366	↓	↓
Precoat-standard (figs. 7 to 12)	400	204	120	55	1000	305		
Precoat (fig. 13)	600 to 800	316 to 427	100 to 110	45 to 50	1100 to 1200	336 to 366		
Continuous coat (fig. 14)	600 to 800	316 to 427	90 to 100	41 to 45	1050 to 1150	320 to 350	25	.17

TABLE III. - STRESS-CORROSION EXPOSURE CONDITIONS

[Exposure temperature, 600° to 800° F (316° to 427° C).]

Type of experiment	Airflow							
	Mass flow		Velocity		Pressure		Dewpoint	
	lb/hr	kg/hr	ft/sec	m/sec	psia	MN/m^2	°F	°C
Standard (figs. 7, 8, 12, and 13)	100 to 110	45 to 50	1100 to 1200	336 to 366	30	0.21	-120	-84
Static air (fig. 9)	---	---	---	---	Ambient	Ambient	Ambient	Ambient
Air pressure (fig. 10)	124 to 132	56 to 60	800 to 900	240 to 270	52	.36	-120	-84
Air dewpoint (fig. 11)	100 to 110	45 to 50	1100 to 1200	336 to 366	30	.21	40	4
Continuous deposition (fig. 14)	90 to 100	41 to 45	1050 to 1150	320 to 350	25	.17	-120	-84

TABLE IV. - SUMMARY OF BASELINE THRESHOLD DATA FOR AS-MACHINED SPECIMENS OF Ti-8Al-1Mo-1V ALLOY (FIG. 7)

[No heat-tinted cracks.]

Specimen	Exposure conditions					Tensile test data						Salt coating	
	Temperature		Time, hr	Stress		Ultimate		Fracture		Reduction in area, percent	Elongation percent	$mg/in.^2$	mg/cm^2
	°F	°C		ksi	MN/m^2	ksi	MN/m^2	ksi	MN/m^2				
58	600	316	96	50	345	147	1013	132	909	34	17	0.28	0.043
56	↓	↓	96	60	414	147	1013	132	909	33	17	.11	.017
73			96	70	482	148	1020	132	909	33	19	.20	.031
102			94	70	482	149	1027	134	923	33	17	.10	.015
72			96	80	551	150	1034	136	937	32	18	.13	.020
[a]225			↓	80	551	147	1013	132	909	32	19	.24	.037
53				90	620	155	1069	155	1069	11	10	.17	.026
[a]226				90	620	149	1027	139	958	30	17	.41	.064
[a]253	↓	↓		100	689	150	1034	150	1034	10	8	.28	.043
69	700	371	↓	40	276	148	1020	132	909	38	17	.20	.031
43	↓	↓	95	50	345	149	1027	131	902	35	18	.13	.020
[a]242			96	50	345	151	1041	137	944	30	19	.53	.082
70			↓	60	414	153	1055	153	1055	14	9	.20	.031
[a]247				60	414	149	1027	138	951	28	19	.38	.059
[a]248	↓	↓		70	482	149	1027	149	1027	16	10	.23	.036
30	800	427		10	69	152	1048	150	1034	19	14	.16	.025
[a]239	↓	↓		10	69	150	1034	144	992	27	17	.41	.064
36				20	138	148	1020	146	1006	19	14	.23	.036
[a]231				20	138	149	1027	139	958	27	18	.17	.026
[a]234				30	207	153	1055	153	1055	11	7	.42	.065
18			↓	50	345	152	1048	152	1048	10	8	.09	.014
12	↓	↓	112	50	345	151	1041	150	1034	7	6	.17	.026

[a]Separate batch of specimens, machined and tested 1 year later.

TABLE V. - SPECIMEN-SURFACE-CONDITION THRESHOLD DATA

Specimen	Exposure conditions					Tensile test data						Salt coating		Heat-tinted cracks
	Temperature		Time, hr	Stress		Ultimate		Fracture		Reduction in area, percent	Elongation, percent	$mg/in.^2$	mg/cm^2	
	°F	°C		ksi	MN/m^2	ksi	MN/m^2	ksi	MN/m^2					
Stress relieved at 1200° F (649° C) for 30 min (no figure)														
244	600	316	96	20	138	145	999	145	999	7	5	0.74	0.11	---
223	↓	↓	95	30	207	148	1020	148	1020	16	15	.82	.13	---
141			95	30	207	156	1075	156	1075	11	9	.31	.048	---
124			95	50	345	152	1048	152	1048	10	9	.27	.042	---
154	↓	↓	94	70	482	147	1013	147	1013	8	2	.78	.12	Yes
142	700	371	95	20	138	155	1069	150	1034	21	14	.17	.026	---
158	700	371	98	40	276	150	1034	149	1027	15	11	.12	.019	---
Chemically milled (fig. 8)														
135	600	316	96	30	207	146	1006	135	930	30	18	0.53	0.082	---
289			95	30	207	145	999	134	923	30	18	.47	.073	---
[a]292			96	30	207	147	1013	134	923	32	20	.26	.040	---
[b]296			96	40	276	151	1041	151	1041	12	10	.54	.084	---
[c]303			96	40	276	148	1020	147	1013	16	10	.42	.065	---
[d]304			94	40	276	147	1013	147	1013	12	9	.41	.064	---
128	↓	↓	96	50	345	143	985	143	985	5	7	.15	.023	Yes
311	700	371	95	20	138	147	1013	134	923	30	16	.81	.13	---
281			96	30	207	148	1020	139	958	24	14	.35	.054	---
288			96	40	276	148	1020	148	1020	17	11	.38	.059	---
285	↓	↓	96	50	345	147	1013	147	1013	12	8	.54	.084	Yes
299	800	427	95	10	69	149	1027	147	1013	19	14	.53	.082	---
290	800	427	96	30	207	148	1020	148	1020	13	13	.41	.064	---
316	800	427	96	40	276	140	965	140	965	8	2	.41	.064	Yes

[a]Chemically milled 0.002 in. (0.005 cm).
[b]Chemically milled 0.0005 in. (0.001 cm).
[c]Exposed at room temperature for 4 weeks.
[d]Exposed at 400° F (204° C) for 2 hours.

All other specimens tested soon after chemical milling 0.001 in. (0.002 cm).

TABLE VI. - STATIC-AIR-ENVIRONMENT THRESHOLD DATA

[No heat-tinted cracks.]

Specimen	Exposure conditions					Tensile test data						Salt coating	
	Temperature		Time, hr	Stress		Ultimate		Fracture		Reduction in area, percent	Elongation, percent	$mg/in.^2$	mg/cm^2
	^oF	^oC		ksi	MN/m^2	ksi	MN/m^2	ksi	MN/m2				
As-machined (fig. 9)													
155	600	316	95	50	345	153	1055	144	992	29	16	0.39	0.061
310	600	316	96	60	414	148	1020	135	930	32	16	.99	.15
90	600	316	↓	70	482	148	1020	148	1020	9	5	.71	.11
144	700	371	↓	30	207	148	1020	132	909	35	17	.19	.029
152	↓	↓	↓	30	207	149	1027	134	923	35	18	10.5	1.6
314	↓	↓	↓	40	276	153	1055	136	937	31	16	.92	.14
83	↓	↓	97	50	345	152	1048	152	1048	9	5	.86	.13
156	800	427	96	10	69	151	1041	151	1041	11	7	.60	.093
Chemically milled (no figure)													
284	600	316	96	30	207	146	1006	130	895	34	19	0.46	0.071
313	600	316	96	30	207	147	1013	131	902	34	19	.53	.082

TABLE VII. - INCREASED-AIR-PRESSURE THRESHOLD DATA

[No heat-tinted cracks.]

Specimen	Exposure conditions					Tensile test data						Salt coating	
	Temperature		Time, hr	Stress		Ultimate		Fracture		Reduction in area, percent	Elongation, percent	$mg/in.^2$	mg/cm^2
	°F	°C		ksi	MN/m^2	ksi	MN/m^2	ksi	MN/m^2				
As-machined (fig. 10)													
133	600	316	96	70	482	148	1020	134	923	30	18	0.45	0.070
149	↓	↓	↓	90	620	148	1020	134	923	32	18	.36	.056
125				110	758	151	1041	136	937	31	16	.16	.025
243				110	758	153	1055	138	951	31	16	.54	.084
251	700	371	94	50	345	148	1020	135	930	32	19	.50	.078
150	700	371	95	60	414	151	1041	145	999	25	15	.57	.088
139	700	371	99	70	482	151	1041	150	1034	15	11	.25	.039
258	800	427	94	10	69	151	1041	142	978	26	19	.14	.022
240	800	427	96	20	138	152	1048	151	1041	15	14	.21	.033
Chemically milled (no figure)													
309	600	316	96	40	276	146	1006	133	916	33	18	0.54	0.084
286	600	316	95	50	345	146	1006	146	1007	17	11	.61	.095

TABLE VIII. - INCREASED-AIR-DEWPOINT THRESHOLD DATA

Specimen	Exposure conditions					Tensile test data						Salt coating		Heat-tinted cracks
	Temperature		Time, hr	Stress		Ultimate		Fracture		Reduction in area, percent	Elongation, percent	$mg/in.^2$	mg/cm^2	
	°F	°C		ksi	MN/m^2	ksi	MN/m^2	ksi	MN/m^2					
As-machined (fig. 11)														
92	600	316	97	80	551	152	1048	138	951	31	16	0.71	0.11	---
109	↓	↓	95	90	620	153	1055	142	978	27	20	.34	.053	---
151			93	100	689	152	1048	138	951	34	19	.36	.056	---
138			96	110	758	151	1041	149	1027	19	11	.91	.14	Yes
146	700	371	95	30	207	150	1034	139	958	29	18	---	----	---
148	↓	↓	93	40	276	151	1041	148	1020	22	17	.32	.050	---
103			95	50	345	152	1048	136	937	30	15	.05	.008	---
126			96	50	345	150	1034	150	1034	11	6	.54	.084	---
85			96	60	414	133	916	133	916	8	1	.74	.11	Yes
122	800	427	97	10	69	150	1034	134	923	35	19	.08	.012	---
224	800	427	97	20	138	152	1048	152	1048	17	14	.27	.042	---
Chemically milled (no figure)														
301	600	316	96	30	207	147	1013	139	958	26	18	0.50	0.080	---

TABLE IX. - HEAVY-SALT-CONCENTRATION THRESHOLD DATA

Specimen	Exposure conditions					Tensile test data						Salt coating		Heat-tinted cracks
	Temperature		Time, hr	Stress		Ultimate		Fracture		Reduction in area, percent	Elongation, percent	$mg/in.^2$	mg/cm^2	
	°F	°C		ksi	MN/m^2	ksi	MN/m^2	ksi	MN/m^2					
As-machined (fig. 12)														
94	600	316	95	80	551	150	1034	138	951	33	19	0.80	0.12	---
108	600	316	99	80	551	153	1055	133	916	33	17	2.6	.40	---
119	600	316	99	90	620	152	1048	145	999	24	14	3.9	.60	---
101	700	371	96	50	345	151	1041	136	937	31	16	5.9	.92	---
118	700	371	101	60	414	151	1041	141	972	27	17	2.9	.45	---
99	700	371	93	70	482	143	985	143	985	8	0	1.5	.23	Yes
132	800	427	97	10	69	148	1020	140	965	27	17	5.2	.81	---
37	800	427	96	20	138	148	1020	148	1020	16	13	.4	.06	---
Chemically milled (no figure)														
318	600	316	95	30	207	146	1006	144	992	21	16	1.8	0.28	---

TABLE X. - ELEVATED-TEMPERATURE-SALT-DEPOSITION THRESHOLD DATA

Specimen	Exposure conditions					Tensile test data						Salt coating		Heat-tinted cracks
	Temperature		Time, hr	Stress		Ultimate		Fracture		Reduction in area, percent	Elongation, percent	$mg/in.^2$	mg/cm^2	
	°F	°C		ksi	MN/m^2	ksi	MN/m^2	ksi	MN/m^2					
As-machined (fig. 13)														
131	600	316	95	90	620	147	1013	131	902	36	18	0.28	0.043	---
160	600	316	90	100	689	153	1055	144	992	29	17	.90	.14	---
116	600	316	93	110	758	151	1041	150	1034	6	3	.66	.10	Yes
113	700	371	95	60	414	155	1069	137	944	32	17	.47	.073	---
89	700	371	95	70	482	150	1034	134	923	34	17	.55	.085	---
87	700	371	95	80	551	150	1034	145	999	22	14	.56	.087	---
120	800	427	96	10	69	156	1075	156	1075	11	6	.07	.011	---
91	↓	↓	95	30	207	146	1006	146	1006	14	8	.23	.036	---
110			95	40	276	145	999	145	999	13	7	.12	.019	---
98			93	50	345	148	1020	142	978	25	17	.46	.071	---
111			96	50	345	153	1055	153	1055	16	8	.44	.068	Yes
97			93	60	414	145	999	145	999	7	3	.51	.079	Yes
Chemically milled (no figure)														
282	600	316	94	40	276	149	1027	132	909	36	19	0.10	0.16	---
300	600	316	95	40	276	147	1013	133	916	34	19	.45	.70	---
293	600	316	95	50	345	144	992	144	992	9	5	.60	.93	---

TABLE XI. - CONTINUOUS-SALT-DEPOSITION THRESHOLD DATA FOR AS-MACHINED SPECIMENS (FIG. 14)

[No heat-tinted cracks.]

Specimen	Exposure conditions					Tensile test data						Salt coating	
	Temperature		Time, hr	Stress		Ultimate		Fracture		Reduction in area, percent	Elongation, percent	$mg/in.^2$	mg/cm^2
	°F	°C		ksi	MN/m^2	ksi	MN/m^2	ksi	MN/m^2				
55	600	316	96	70	482	153	1055	138	951	30	17	7.4	1.1
64	↓	↓	97	90	620	147	1013	131	902	34	18	.88	.14
57			97	100	689	152	1048	141	972	29	15	.37	.057
44			112	110	758	149	1027	127	875	35	15	.31	.048
112			96	115	792	157	1082	138	951	31	16	1.0	.15
117	700	371	98	50	345	155	1069	142	978	29	19	.91	.14
86	700	371	94	60	414	147	1013	129	889	35	19	1.0	.15
47	700	371	96	70	482	151	1041	151	1041	10	5	1.1	.17
41	800	427	95	30	207	150	1034	133	916	34	18	.71	.11
48	↓	↓	112	40	276	153	1055	138	951	33	19	.59	.092
81			93	50	345	148	1020	132	909	36	17	.43	.067
50			96	50	345	151	1041	---	---	25	19	.56	.087
52			96	60	414	153	1055	137	944	34	19	.50	.078
82			96	60	414	148	1020	148	1020	8	4	.41	.064
104			97	70	482	153	1055	153	1055	8	2	.30	.046

TABLE XII. - INCREASED-EXPOSURE-TIME THRESHOLD DATA FOR AS-MACHINED SPECIMENS (NO FIG.)

[No heat-tinted cracks.]

Specimen	Exposure conditions					Tensile test data						Salt coating	
	Temperature		Time, hr	Stress		Ultimate		Fracture		Reduction in area, percent	Elongation, percent	$mg/in.^2$	mg/cm^2
	°F	°C		ksi	MN/m^2	ksi	MN/m^2	ksi	MN/m^2				
143	600	316	238	50	345	150	1034	138	951	29	17	0.37	0.057
136	600	316	234	70	482	153	1055	153	1055	11	6	.42	.065

NASA-Langley, 1969 —— 17 E-5212

"The aeronautical and space activities of the United States shall be conducted so as to contribute . . . to the expansion of human knowledge of phenomena in the atmosphere and space. The Administration shall provide for the widest practicable and appropriate dissemination of information concerning its activities and the results thereof."

—NATIONAL AERONAUTICS AND SPACE ACT OF 1958

NASA SCIENTIFIC AND TECHNICAL PUBLICATIONS

TECHNICAL REPORTS: Scientific and technical information considered important, complete, and a lasting contribution to existing knowledge.

TECHNICAL NOTES: Information less broad in scope but nevertheless of importance as a contribution to existing knowledge.

TECHNICAL MEMORANDUMS: Information receiving limited distribution because of preliminary data, security classification, or other reasons.

CONTRACTOR REPORTS: Scientific and technical information generated under a NASA contract or grant and considered an important contribution to existing knowledge.

TECHNICAL TRANSLATIONS: Information published in a foreign language considered to merit NASA distribution in English.

SPECIAL PUBLICATIONS: Information derived from or of value to NASA activities. Publications include conference proceedings, monographs, data compilations, handbooks, sourcebooks, and special bibliographies.

TECHNOLOGY UTILIZATION PUBLICATIONS: Information on technology used by NASA that may be of particular interest in commercial and other non-aerospace applications. Publications include Tech Briefs, Technology Utilization Reports and Notes, and Technology Surveys.

Details on the availability of these publications may be obtained from:

SCIENTIFIC AND TECHNICAL INFORMATION DIVISION

NATIONAL AERONAUTICS AND SPACE ADMINISTRATION

Washington, D.C. 20546